Article

Assessment of Beach Slope and Sediment Grain Size Anywhere in the World: Review of Existing Formulae, Integration of Tidal Influence, and Perspectives from Satellite Observations

Amélie Arias [1], Rafael Almar [1,*], Vincent Regard [2], Erwin W. J. Bergsma [3], Bruno Castelle [4] and Thierry Garlan [5]

[1] Laboratoire D'études en Géophysique et Océanographie Spatiales (LEGOS, Université de Toulouse/CNES/CNRS/IRD), 31400 Toulouse, France; amelie.arias@univ-tlse3.fr
[2] Géosciences Environnement Toulouse (GET, CNRS/Université de Toulouse/IRD/CNES), 31400 Toulouse, France; vincent.regard@get.omp.eu
[3] French Space Agency (CNES), Earth Observation Lab, 31400 Toulouse, France; erwin.bergsma@cnes.fr
[4] Environnements et Paléoenvironnements Océaniques et Continentaux (EPOC, University of Bordeaux/CNRS), 33615 Pessac, France; bruno.castelle@u-bordeaux.fr
[5] Service Hydrographique et Océanographique de la Marine (SHOM), 29200 Brest, France; thierry29.garlan@gmail.com
* Correspondence: rafael.almar@ird.fr

Abstract: Grain size and beach slope are critical factors in coastal science and management. However, it is difficult to have information on their distribution everywhere in the world, as most of the coast has never been documented. For many applications, it is essential to have at least a rough estimate when local field measurements are not available. Here, we review the existing prediction formulas relating beach slope to grain size and wave conditions, using publicly available global datasets and comparing them with a benchmark dataset of ground measurements from different authors worldwide. Uncertainties arise from the input parameters, in particular coastal waves, a key parameter of all formulae, but also from empirical coefficients that are undocumented or inaccessible with the global dataset. Despite the recognized importance of tides, they are often overlooked in formulae relating beach slope to sediment grain size. We therefore present an improved formulation that incorporates tidal effects. Although satellites offer a promising alternative to predictive formulae for direct estimation of beach slope and grain size, the current accuracy and methodologies of satellite data are insufficient for global applications. Continued advances in satellite missions, including higher resolution and revisit frequency, as well as new sensors, are essential to improve predictive capabilities and facilitate wider implementation.

Keywords: beach slope; sediment grain size; satellite optical imagery; waves; tide

1. Introduction

Coastal areas are dynamic environments that undergo continuous changes due to natural processes and human activities [1]. Understanding and predicting beach evolution is essential for effective coastal management, risk assessment, and sustainable development. Among the various parameters of beach morphology, beach slope is particularly critical [2]. It significantly influences the type and intensity of wave breaking (from spilling to surging to plunging [3–5]), which is crucial for beach safety and lifeguarding [6]. Beach slope also affects the reflection of gravity and infragravity waves at the shore [7] and is a key parameter in many empirical and semi-empirical formulas used, for example, to estimate

wave run-up [8] and total water level [9,10] or longshore drift [11]. These formulas typically assume that beach slope is a fixed, time-invariant parameter. However, beach slope is not homogeneous along the beach profile and continuously evolves in response to storm, seasonal, and interannual variations in incident wave conditions. This temporal and spatial variability of beach slope remains poorly understood.

The median particle diameter d_{50} is a key parameter (Figure 1) because it influences the ability of particles to be transported by hydrodynamic agents [12–14]. Several morphodynamic or one-line shoreline models, such as the Coastal Evolution Model (CEM) proposed by [15] and the XBeach model, as well as the ShorelineS model created by [16,17], rely on d_{50}. In these models, coastal changes are induced by the longshore transport produced by waves, which can be calculated using various formulations [11,18–20]. Dimensional analysis has shown that the longshore transport rate is a function of a combination of wave steepness, beach slope, wave angle, and relative grain size in the breaking zone [11]. Larger particles require more energy to be transported and are typically found in high-energy environments such as fast-flowing rivers or coastal areas [18]. In contrast, finer particles are transported by weaker currents or winds, leading to their accumulation in low-energy environments such as lakes or deep-sea basins.

Figure 1. Illustration of the wide variety of sediment grain size along world beaches (Photos from E. Anthony at Grand Popo, Benin, left, and A. Arias at Oleron island, France, right).

Linking sediment grain size and beach slope is critical because it provides insight into sedimentary processes and coastal dynamics. As demonstrated by [12], the beach-face slope is correlated with the sediment median diameter. Over the years, researchers have explored this relationship, resulting in empirical formulas that relate beach-face slope to grain size [21–24]. However, many of these formulas exclude tidal influences, which are critical in shaping beach morphology (e.g., [25]). Tidal effects redistribute wave energy over a larger area, resulting in gentler slopes and the formation of intertidal features [26]. Conversely, low tidal ranges concentrate wave energy, creating steeper slopes and localized erosion. To better understand the links between d_{50} and beach slope, large datasets spanning the entire dissipative-reflective beach state continuum are required. Collecting such datasets through in situ measurements is challenging. However, satellite remote sensing offers a promising alternative for large-scale data acquisition and analysis.

Recent advances in satellite technology have enabled the integration of satellite data into coastal evolution models, providing regional to global datasets on waterline position, coastal topobathymetry [27], and more [28–31]. Satellites offer long-term information and access to remote or poorly studied areas. However, while satellite images have been used to monitor changes in coastal morphology and sediment distribution [32,33], their

application to deriving beach slope and median grain size has been limited. Notable contributions in this area include the work of [34] on satellite-derived beach slope and [35] on satellite-derived beach grain size.

In this paper we aim to pragmatically test the existing options for inferring beach slope and grain size, potentially anywhere in the world, as a first pass. We first review the empirical formulae relating beach slope to grain size and test their application against in situ measurements using publicly available global reanalysis datasets. Next, we propose a modification of existing formulations to include tidal range. We then evaluate the accuracy of direct satellite-derived slope estimates and use these modified formulas to infer beach grain size. Finally, we discuss the uncertainties of the formulas, our approach using global datasets and satellite techniques, and identify opportunities for future improvement.

2. Data and Methods

We use ground data from existing literature and globally available wave information (Figure 2—Appendix A) to compare the performance of commonly used empirical formulas. The selected sites focus exclusively on open coast beaches, where ERA5 data reliably measures inshore wave conditions. This approach avoids the inaccuracies that could arise in sheltered and/or embayed coasts, where ERA5 may not represent near-breaking wave conditions. Across our 20 study sites, grain size varies widely, with fine particles around 0.18 mm (5th percentile), typical grains around 0.35 mm (median) and coarse particles up to 1.68 mm (95th percentile). Beach slopes also show considerable variation, ranging from gently sloping beaches at 0.02 to steeper slopes at 0.15, with an average of around 0.09.
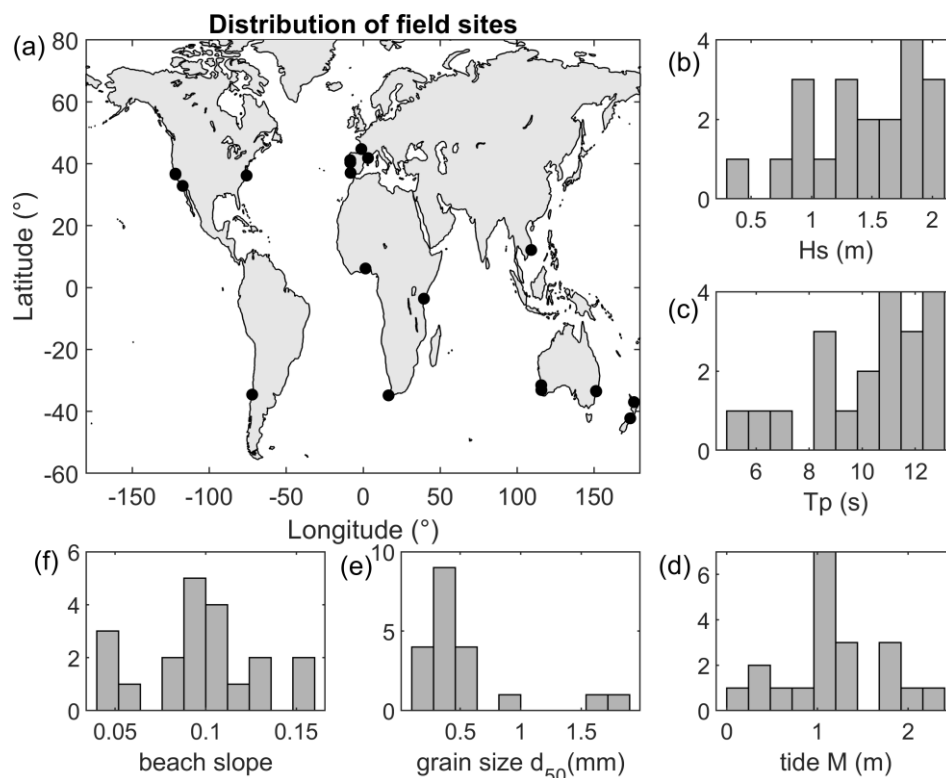

Figure 2. Location of the studied field sites (black circles) in (**a**), with the distribution of formula parameters, hydrodynamic forcing from global numerical models, wave (**b**) *Hs* and (**c**) *Tp*, (**d**) tidal range (*M*), and locally measured (**e**) grain size and (**f**) beach slope.

The significant wave height (*Hs*) and peak period (*Tp*) for each point considered in this study are extracted from the ECMWF ERA5 reanalysis. These parameters are extracted on a grid of $0.5° \times 0.5°$, with a daily temporal resolution, and averaged over

the 2000–2019 period. *Hs* and *Tp* range from 0.5, 1.4, and 2.0 m, and 5.8, 10.8, and 13 s, for the 5th, median, and 95th percentiles. Noteworthy, *Hb*, required in the formulas, is not available worldwide and would require accurate local wave modelling or in situ observation. Astronomical tides are extracted from the global tide model FES (Finite Element Solution, [36]) at the field sites. The mean tidal range (*M*, computed as 4 times the standard deviation) is computed from hourly resolution over the 1993–2023 period. Tide ranges from 0.2, 1.03, and up to 2.2 for the 5th, median, and 95th percentiles.

Beach slope is estimated on the basis of the tidally varying waterline position following the principle proposed by [33]. The beach slope ($slope_{sat}$) is calculated as the average of the change in elevation over the displacement in the cross-shore position (Equation (1)).

$$slope_{sat} = \overline{\frac{\Delta Z}{\Delta X}} \tag{1}$$

where ΔZ represents the change in sea level anomaly, and ΔX is the cross-shore displacement of the shoreline position. In this study, two types of satellite-derived datasets were utilized, as described in the next two paragraphs.

First, we utilize a global satellite dataset defined by [37], which includes optical-based waterlines and sea level data from altimetry, covering the period from 1993 to 2023. The dataset consists of 14,140 sampling points at 0.27° intervals (with a 500 m alongshore buffer) along the global coastline, which were filtered to retain 3592 points corresponding to sandy beaches, as identified by [38]. For further analysis, we extracted the closest points to the field sites. Waterlines, representing the interface between land and sea surfaces, were determined using the Normalized Difference Water Index (NDWI, [39], derived from Landsat 30 m data in Google Earth Engine (GEE) on a monthly basis. Monthly water levels were approximated from regional sea levels obtained through satellite altimetry time series using the SSALTO/DUACS multi-mission data [40]. Dynamical Atmospheric Corrections (DAC) were acquired from the hourly outputs of the MOG2D-G model [36], which were forced by surface winds and atmospheric pressure from the ERA-5 reanalysis [41].

Second, satellite data, specifically refined Sentinel-2 imagery and instantaneous 10 m SCOWI indexes, were utilized to create a site-specific dataset for more precise local analysis. We adopted methods from the toolkit of [34] to focus on extracting locally specific waterlines using Google Earth Engine (GEE) and processed through the Shoreliner Pipeline [42]. At this finer scale, water levels were approximated using astronomical tides derived from FES2022 [36]. This approach aims to reduce potential inaccuracies associated with relying on a broad, global dataset that may not accurately reflect conditions at the actual field site. Additionally, we applied the principle from [35] to explore whether Sentinel-2-derived shoreline position variability could be used to directly estimate grain size (d_{50_sat}, Equation (2)).

$$d_{50\_sat} = a\overline{\Delta X} \tag{2}$$

3. Results

3.1. Review of Empirical Formulas Linking Beach Slope and Grain Size

Here, we review some existing published empirical formulas, listed in Table 1. These formulas are derived from data, in situ and laboratory (see Table 2), which do not cover the full spectrum of possible values for each parameter. This is why we also describe the type of data and range used to define each formula. Full beach profile formulas Dean's formulas (e.g., [41,43]) are not considered here and included in Table 1 because they focus primarily on equilibrium beach profiles characterized by a concave shape, rather than providing a direct empirical estimate of linear beach slopes. The complexity of comparing

a non-linear, concave profile to these linear models would require detailed justification and an alternative analytical framework, which is beyond the scope of this specific review.

Table 1. Synthesis of the different empirical formulae explored in this work.

Name in This Work and Reference	Empirical Formula for Beach Slope Estimation	Parameters
Sunamura84 [22]	$\tan \beta = 0.12 \left[\frac{d_{50} g T p^2}{H_b} \right]^{0.5}$	H_b Breaking wave height g Acceleration due to gravity d_{50} Median grain size Tp Wave period
Reis_Gama10 [23]	$\tan \beta = 0.9 * H_b^{-10/3} * d_{50}^{4/3}$	H_b Breaking wave height d_{50} Median grain size
Kim14 [44]	$\tan \beta = 0.332 * Tp^{-0.416} * d_{50}^{0.122}$	d_{50} Median grain size Tp Wave period
Bujan19 [45]	$\tan \beta = -0.154(d_{50} - 0.125)^{-0.145} + 0.268$	d_{50} Median grain size

Table 2. Range of values and type of source (in situ or laboratory) on which formulas have been established and/or validated. These formulas do not account for tide which is not documented here.

Formula	Range of In Situ Variable Values	Range of Laboratory Variable Values
Sunamura84 [22]	H_b [0.8–1.6 m] d_{50} [0.2–1.0 mm] Tp [6–12 s] $\tan \beta$ [0.01–0.3]	d_{50} [0.2 and 1 mm] $\tan \beta$[0.1 to 0.7]
Reis_Gama10 [23]	H_b [0.3–3.2 m] d_{50} [0.18–0.65 mm] S = 0.9 (sphericity)	Not applied
Kim14 [44]	Not applied	d_{50} [0.2–0.7 mm] Tp [1.5–9 s]
Bujan19 [45]	d_{50} [0.07–770 mm]; 10–90 percentile = [0.2–25 mm] $\tan \beta$ [0.01–0.8]; 10–90 percentile = [0.025–0.18 mm]	Not applied

In 1975, [22] introduced a "static" formula based on earlier studies by Kemp and Plinston (1968). It assumes that the beach slope stabilizes instantaneously under wave action and is a function of the dimensionless parameter $H_b / g^{0.5} d_{50}^{0.5} Tp$, where H_b is wave height at breaker, g is gravitational acceleration, d_{50} the median grain size, and T is wave period. This formula has been refined using laboratory and field data, yielding slopes ranging from 0.1 to 0.7 (laboratory) and 0.01 to 0.3 (field), with grain sizes between 0.2 and 1 mm. Although the formula captured the relationship between beach parameters and slope, significant data scatter was found, probably due to the static slope assumption. In 1984, Ref. [22] (referred to after as Sunamura84) tested the dependence of slope on $H_b / g^{0.5} d_{50}^{0.5} Tp$ using laboratory and field data and again found large scatter. This overdispersion was attributed to factors such as variations in wave data, errors in slope measurement, and difficulties in obtaining accurate wave heights at breaking points.

Ref. [23] developed a model, hereafter referred to as Reis_Gama10, to describe the movement of waves as they advance and retreat along the beach face (swash), incorporating both surface flow and flow through the porous sand bed, which has an average porosity of 0.35. The permeability of this sand bed, which is influenced by the size and sphericity of the sand grains (0.9 for beach sand), is determined using the Kozeny–Carmán

equation. Ref. [23] applied the Constructal Law, as introduced by [45], and found that the beach face slope varies with $H^{3/4}$ and $d_{50}{}^{4/3}$. Ultimately, they derived the relationship: $\tan\beta = E * H_s^{-10/3} * d_{50}^{4/3}$ where E is a scaling coefficient determined by field conditions, including grain sphericity, porosity, and fluid viscosity [44].

Ref. [44] reviewed various beach slope equations to identify weaknesses and refine them for more robust predictions. They developed a general equation, Kim14, applicable to all coastal types, assuming no tide, equilibrium beach slope, normal wave direction, uniform grain size, and flat onshore berms. Using laboratory data, they derived an empirical formula relating beach slope to wave parameters. Ref. [44] concluded that while wave height affects the width of the bed profile, wave period has a significant effect on bed morphology. They proposed an empirical formula for equilibrium beach slope: $\tan\beta = cTp^m d_{50}^n$, where c, m, and n are empirical coefficients. This formula was calibrated using existing laboratory data and compared with the formulas of Sunamura1984 and Reis_Gama10. However, it was calibrated and tested on a limited range of wave periods (1.5–9 s) and mean grain sizes (0.2–0.7 mm).

Ref. [45] sought a formula that would work for a wider range of sediment sizes. To do this, they compiled 2144 measurements of beach face slope with grain size records from the literature and assumed that this relationship could be described by a power law function. This formula, Bujan19 (Table 1), is satisfactory for sediment sizes smaller than cobble ($d_{50} < 64$ mm). This value represents a threshold above which another formula must be found, especially for ridges.

3.2. Test of Formulas: Key Differences and Application

In terms of range of applicability for Bujan19, there are two domains, whether finer or coarser than coarse sands (0.5–1 mm). Sunamura84 is valid for coarse sediment, Reis_Gama10 works for fine sediment, while Bujan19 should work for all grain sizes up to cobbles. Kim14 has too small a range to be useful for us. In the following we decide to only work on fine to intermediate sediment typical for most of the world's beaches (see observation distribution on Figure 3), as the physics for coarse sediment may be different.
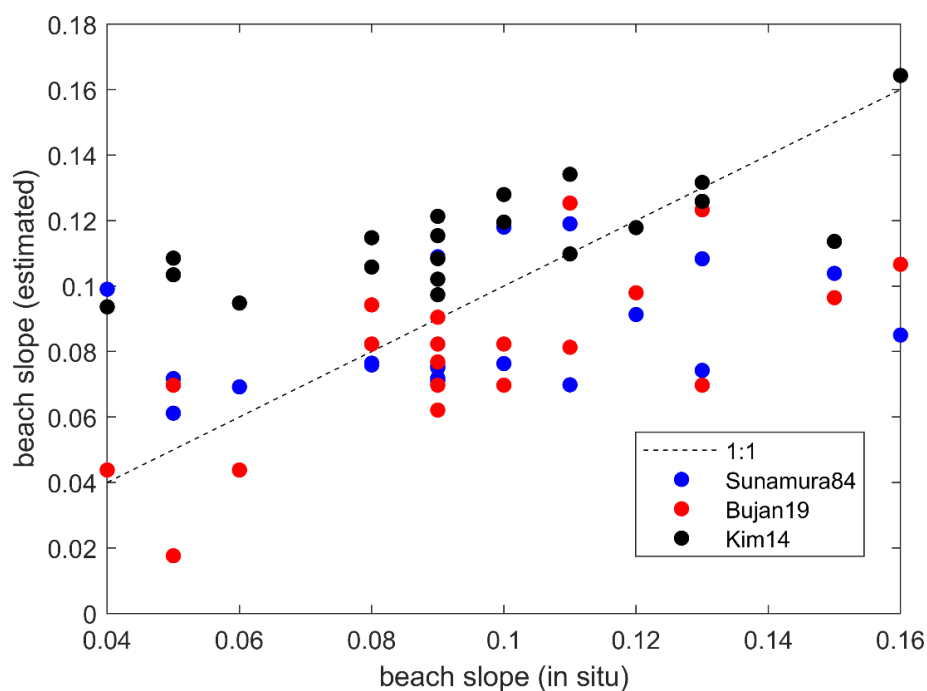

Figure 3. Relationship between in situ and derived beach face slope for the validation sites, using various formulas.

To assess whether these formulas accurately describe natural systems across a range of grain sizes, we use ground data and globally available wave information (Figure 1—Appendix A) to perform a comparison of the performance. The results in relation to our validation dataset are shown in Figure 3. Among the empirical formulas considered, Bujan19, Sunamura84, and Kim14 are in decreasing order of performance in predicting grain size with our field data across the entire sediment size spectrum. In contrast, the Reis_Gama10 formula is the least performing equation, mainly out of range and therefore not shown here. Interestingly, Bujan19 seems to perform better while it is the one that depends on the lesser parameters, in particular not the waves.

The performance of Bujan19 is based uniquely on grain size, and adding more input variable does not necessarily mean a better score (Table 3). To assess the importance of the parameters to be accounted for to estimate beach slope, we conducted a multilinear regression and computed the fraction explained by each parameter. In our ground-based dataset, where the spatio-temporal variability of coastal variables is not fully captured due to single-point or one-time measurements or, in contrast, time-averaged values, combining grain size, wave parameters (Hs, Tp), and median tidal range (M) explains 52% (R^2) of the total variance in beach slope. Waves (Hs and Tp together: 48%) result as one of the predominant parameters influencing the slope, followed by grain size (30%) and tide (21%) (Figure 4). Thus, this suggests that it is somehow a good idea to consider unique grain size but indicate that waves and tides both have an important role on beach slope. Not including tide would bring dispersion, as already suggested by previous studies (e.g., [2]). In this sense, Sunamura84 seems to be a good basis to implement the tide effect.

Table 3. Score of the considered formulas when applied to our natural beaches dataset.

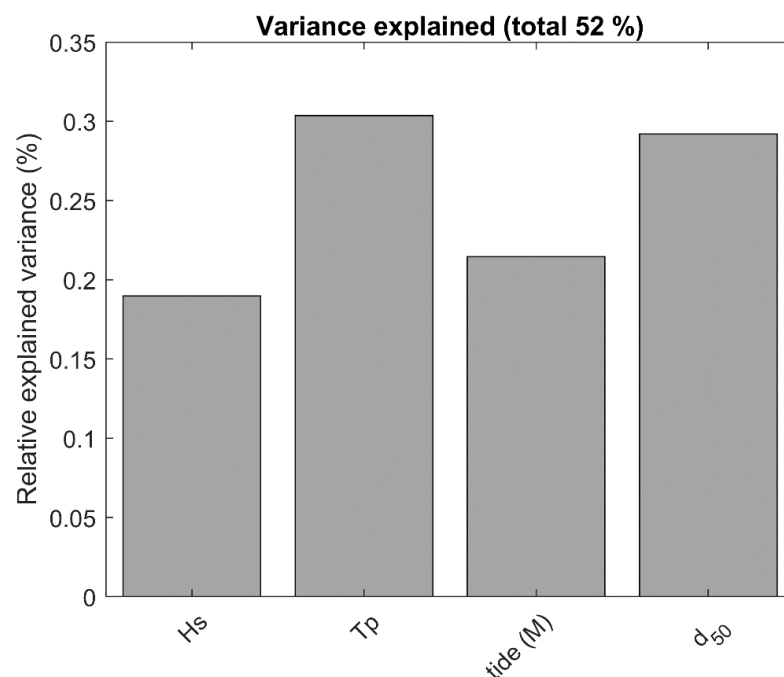| Formula	RMSE	Correlation
Sunamura84 [22]	0.03	0.48
Reis_Gama10 [23]	0.09	<0.2
Kim14 [44]	0.03	0.71
Bujan19 [45]	0.02	0.69

Figure 4. Explained fraction of the total reconstructed signal (52%) of the grain size variability, considering a multilinear model.

3.3. An Adaptation Needed to Include Tidal Influence

Our data count with: 13% of sites where *Hs* is large relative to the tidal range *M* (*Hs* > 2x*M*) and can be defined as wave-dominated; 39% of sites where the tidal range is large (2x) relative to *Hs* and can be defined as tide-dominated; and 47% of sites present *Hs* and tidal range of comparable magnitude (2*Hs* > *M* > *Hs*/2) and can be considered as mixed. In order to address the influence of tide on the links between grain size and beach slope, which was disregarded in previous studies, we extracted the median astronomical tidal range (*M*) from the global tide model FES (Finite Element Solution, Carrere et al., 2014) at all field sites (see Data Section). To integrate tidal range into beach slope models, semi-empirical relationships can be used, such as the integration of the tidal range (*M*) into the formulation (Equation (3)).

$$Hs_{\_tide} = Hs * \left(1 + \frac{M}{Hs}\right) = Hs(1 + RTR) \tag{3}$$

where *RTR* is the Relative Tidal Range introduced by Masselink and Short (1993)—Equation (4):

$$RTR = M/Hs \tag{4}$$

In Equation (3), the tidally modulated *Hs* indicates that this hydrodynamic term $Hs_{\_tide}$ is unchanged and is similar to *Hs* when tidal range tends to zero but is artificially increased up to reaching tidal range when *Hs* is small and tidal range is large. $Hs_{\_tide}$ can be re-injected in formulas depending on *Hs*, here Sunamura84, proposing a modified formulation (Equation (5)).

$$\tan \beta = 0.12 \left[\frac{d_{50}gT^2}{H_b(1 + RTR)}\right]^{0.5} \tag{5}$$

The RMSE then reduces to 0.02, and the correlation increases to 0.66, showing the influence of tide on reshaping the beach slope (Figure 5).
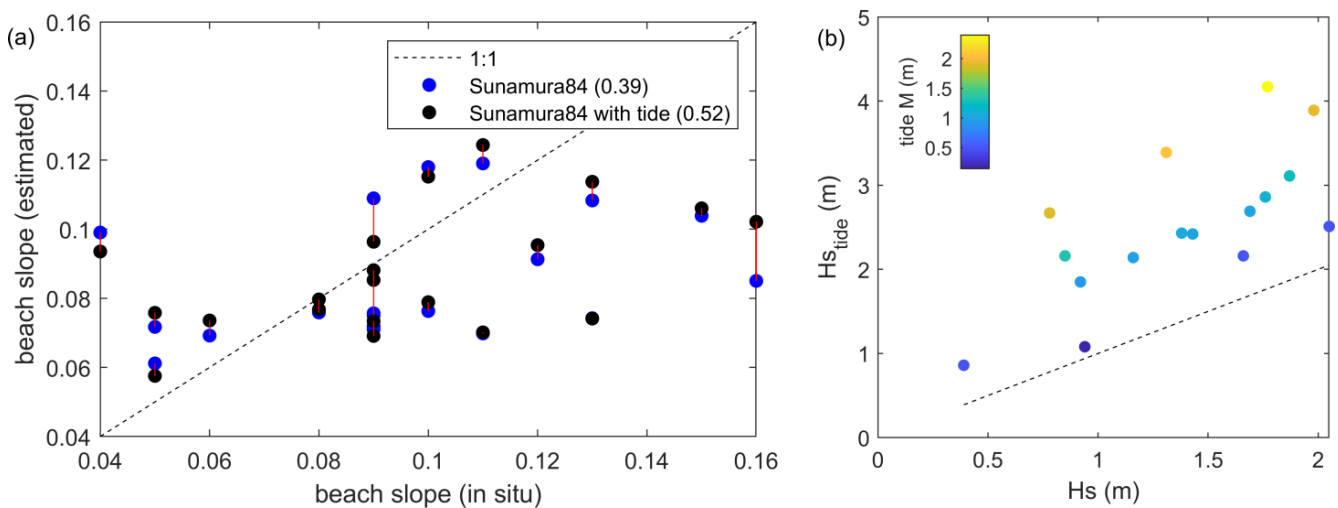

Figure 5. (**a**) Observed versus predicted beach slopes considering the Sunnamura84 formula and the tidally modified expression of *Hs* and (**b**) the departure of the hydrodynamic parameter $Hs_{\_tide}$ influenced by tidal range from original Hs (i.e., no tidal range gives $Hs_{\_tide}$ = *Hs* over the 1:1 line).

4. The Satellite View: From Beach Slope Estimation to Beach Grain Size

4.1. Beach Slope Estimation

Using the global and site-specific local datasets we extract waterlines and sea level. From the global monthly and coarse dataset, the calculation of beach slope (Figure 6a) yielded a Root Mean Square Error (RMSE) of 0.03 and a correlation of 0.48 with ground-truth data, indicating a signal-to-noise ratio of 1.5, indicating not only a possible use for a first pass estimation but also that the measurement may still be too noisy and not reliable for precise analyses. Interestingly, the use of site-specific estimation in this case does not yield an improved score with a Root Mean Square Error (RMSE) of 0.06 and a correlation of 0.21 with ground-truth data. The assumption in this approach is also that topography changes are minimal, and shoreline position changes are driven by sea level variations, which we acknowledge is far from reality at sandy beaches.
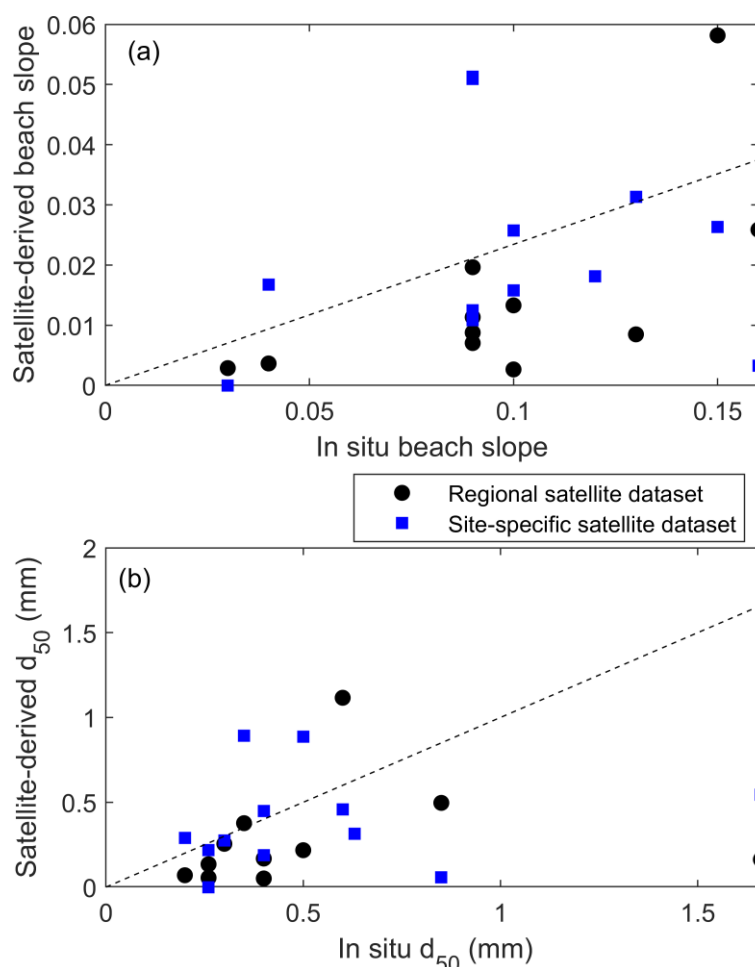

Figure 6. (**a**) Satellite-derived beach slope versus in situ beach slope, and (**b**) relationship between in situ sediment grain size (mm) and derivated beach face slope for the validation sites. The x-axis represents the in situ grain size, and the y-axis represents the calculated beachfront slope using various formulas.

4.2. Grain Size Estimation

Using the global dataset, the correlation between grain size (d_{50_sat}) and cross-shore displacement (ΔX) was found to be 0.3, with a large dispersion (RMSE = 0.4 mm) and a signal-to-noise ratio of 1.2, which is close to 1. These results suggest that the estimation of grain size using shoreline mobility from satellite data is challenging. Using the site-specific satellite-derived data gives very similar scores with a correlation coefficient of 0.27 and

RMSE of 0.36 mm (Figure 6b). In either dataset, the weak performance could be due to either the principle of the method itself or the high local variability of grain size, which may not be well-captured by a regional satellite dataset. Additionally, shoreline mobility might be influenced by factors more complex than grain size alone.

The analysis of grain size and beach slope revealed that both regional and local factors play an important role in shaping coastal beach characteristics. Regional factors such as wave regime, hydrodynamic conditions, sediment supply, and geological context were found to contribute to broad patterns in grain size and slope across different coastal environments. However, local factors such as beach orientation, urbanization, and nearshore dynamics were shown to have a more pronounced influence on finer-scale variations. These local processes often dominate, resulting in substantial variability in beach characteristics over short distances. The combined influence of both scales poses a challenge to accurate generalization of coastal characteristics, as local conditions often alter grain size and slope beyond what regional trends would predict.

5. Discussion

5.1. Common and Original Parameters from Formulas

The main differences between the models of [22,23,44,45] lie in their approaches and data coverage. Ref. [22] uses an empirical, static approach with dimensionless parameters and has significant data scatter due to natural variability. The main limitation is the significant data dispersion and approximations. Ref. [23] use a theoretical, dynamic model that incorporates fine physical properties such as porosity. Its main limitation is the focus on specific physical properties and conditions that are difficult to assess in the field. Ref. [44] empirically refine existing formulas under simplified conditions, focusing on wave period and grain diameter. However, it is calibrated for specific ranges of wave periods and grain sizes, with assumptions that may limit applicability. In contrast, Ref. [45] develop an empirical function from a large dataset, tailored to a wide range of sediment sizes down to cobbles, providing broader applicability. It requires a different formula for larger sediment sizes, especially for ridges. Tide is not explicitly considered in these formulas, as laboratory experiments are conducted without tidal influence. At field sites, the focus is on wave action and grain size, with tidal effects implicitly included within the natural variability and measurement dispersion.

5.2. Uncertainties in the Formula Inputs

Here, we wanted to test the use of beach slope and grain size formulae in natural conditions, which can differ significantly from the optimal ones when they were developed, generally in controlled laboratory conditions. We have also used data that are publicly available anywhere in the world, with the idea of having a first-pass estimation, as we do not believe that these formulas and public coastal datasets are mature enough to be used operationally.

For example, in terms of hydrodynamic drivers, wave data are critical inputs to these formulas. However, waves are typically expressed in terms of breaker height in the beach slope formulae, which is difficult to assess on natural beaches due to complex nearshore transformations. These transformations depend on the local bathymetry, which is not uniformly available around the world. As a result, the use of offshore wave data can lead to significant inaccuracies. In addition, waves are highly variable over time, making it difficult to effectively use time-averaged data in these models. Here, we have used ERA5 offshore wave characteristics, which can differ significantly from the waves at the onset of breaking, which are required in the slope formulae. Similarly, tides and sea levels (altimetric regional sea level and atmospheric surge) are derived from satellite observations

and model reanalysis and are subject to errors that can reach tens of centimeters from coastal sea level [46].

The application of beach slope formulae also depends on the accurate characterization of grain size, which varies greatly in both space and time due to natural forces and sediment heterogeneity (e.g., [47,48]). Spatial variability is observed along the beach profile, with different zones, such as the swash zone, berm, and foreshore, experiencing different hydrodynamic conditions resulting in different grain sizes. Temporal variability is driven by factors, such as seasonal changes, storms, and tidal cycles, which cause shifts in sediment distribution. To accurately predict beach slope, it is critical to measure grain size at multiple locations and depths, capturing both surface and subsurface conditions, and to make repeated measurements over time to account for seasonal and event-driven changes. However, this is not feasible due to the time-consuming nature of the task. Finally, the in situ dataset used here from the literature often lacks slope and grain size time stamps and accurate localization, which is a major uncertainty in our study.

Therefore, both grain size and hydrodynamic inputs are challenges that need to be carefully managed to improve the accuracy of beach slope predictions.

5.3. Challenges in Satellite Estimations

In addition to previous uncertainties, current periodic revisit optical satellite missions have an accuracy of tens of meters, which at best gives an accuracy of tens of meters on the shoreline, particularly for flat beaches [34], even if subpixel accuracy can now be reached (e.g., [36]).

A study by [35] showed some potential in correlating Sentinel-2-derived shoreline variability with grain size, but much of this variability was attributed to local conditions such as beach morphology and localized sediment inputs. In this case, regional satellite datasets have limitations in explaining grain size variability due to the dominance of local processes at finer scales, highlighting the difficulty of generalizing grain size patterns from regional data alone. The satellite-derived estimation of beach slope and grain size highlights the difficulty of capturing coastal characteristics at different spatial scales. While regional factors such as wave energy regime, sediment supply due to geological background, and large-scale tidal characteristics can explain broad trends in both slope and grain size, local processes often dominate finer-scale variations in space and time [2,49]. In our study, the regional and monthly dataset provided reliable estimates of beach slope compared to the site-specific local approach, which is more prone to intrinsic noise and uncertainty from stochastic processes (i.e., swash) inherent in a snapshot observation, suggesting that large-scale and slowly evolving patterns and equilibria may be easier to capture with satellite data, capturing general behavior and smoothing out individual discrepancies. However, the weak correlation between grain size and shoreline mobility from both datasets suggests that grain size is influenced by more complex local factors, such as wave transformation, beach morphology, and sediment transport dynamics, which are not easily captured by satellite imagery alone.

Alternatively, direct estimation of beach sediment grain size from satellites has been introduced, based on high-resolution multispectral imagery [31,50,51], texture analysis, and potentially machine learning. However, environmental factors must be carefully considered, and ground truth data are required.

Beaches change over a wide range of spatio-temporal scales, from tidal cycles to interannual changes due to changes in climate regimes and geological factors [1]. While the magnitude of slope change at different timescales varies from site to site, it is very optimistic to define a constant beach slope value for a beach and position on the profile, which is widely carried out in the literature (i.e., values without a time stamp). Although it has been

overlooked due to difficulties in measurement, grain size also varies significantly along the profile and over time. Such fine and fast dynamics are currently out of reach with satellite imagery, even with the regular 5–10-day (clear sky) revisits of the current mission [28,52,53]. Overall, some efforts are still needed to mature the techniques for estimating grain size and also beach slope from satellites, but the sky is clear when considering new high-resolution satellite missions and sensors such as radar [54] and especially SWOT [55].

6. Conclusions

The characterization of grain size and beach slope is crucial for coastal science and management. This study aims to test the ability to derive these parameters as a first pass anywhere in the world with publicly available datasets, from model reanalysis and satellites.

First, we have reviewed numerous published formulae linking beach slope to grain size and wave conditions for the particular aim of deriving these parameters as a first pass, anywhere in the world, with a publicity available dataset from model reanalysis and satellites. Of these parameters, waves are often the least well defined due to their variability and the challenges associated with accurate field measurement. In addition, empirical coefficients, physical properties that influence scaling factors, and thresholds for larger sediment sizes complicate efforts to make accurate and generalizable predictions at a remote site without detailed documentation.

We have also shown that tides have often been excluded from beach slope predictions, despite their significant influence. In a pragmatic way, we have addressed this gap by proposing a formulation (Equation (5)) that incorporates the tidal influence on waves and beach slope, using a benchmark dataset derived from in situ measurements by different authors. This formulation builds on the approach of [22], modifying the hydrodynamic forcing by modulating the significant wave height to account for tidal effects.

By providing data at any location in the world, without dependence on field measurements, satellites offer an attractive alternative for direct estimation compared to these formulae, which depends on uncertain inputs and simplified physics. However, our results show that the current accuracy of satellite data and methods is not yet adequate for global application. Further technical developments and new missions with improved revisit rates and resolution are needed to improve this capability.

Author Contributions: Conceptualization, A.A., V.R. and R.A., Data processing, A.A., R.A., V.R., T.G. and E.W.J.B. Writing—review and editing, all authors. All authors have read and agreed to the published version of the manuscript.

Institutional Review Board Statement: Not applicable.

Informed Consent Statement: Not applicable.

Data Availability Statement: Dataset values used in this study are provided in Appendix A.

Appendix A

Authors	Location	Beach Slope (tan β)	Grain Size (mm)	Hs (m)	Tp (s)	Tidal Range (m)
[56]	Australia	0.10	0.40	1.38	8.91	1.05
[57]	Spain	0.16	0.85	0.94	5.17	0.14
[58]	USA	0.13	1.66	1.87	11.94	1.24

Authors	Location	Beach Slope (tan β)	Grain Size (mm)	*Hs* (m)	*Tp* (s)	Tidal Range (m)
[59]	USA	0.08	0.40	1.87	11.94	1.24
[60]	Australia	0.09	0.40	2.05	13.01	0.46
[61]	New Zealand	0.12	0.63	1.43	10.53	0.99
[62]	South Africa	0.05	0.30	1.76	11.59	1.10
[63]	Australia	0.09	0.26	1.66	12.86	0.50
[64]	New Zealand	0.11	1.82	1.43	10.53	0.99
[65]	Kenya	0.05	0.16	1.31	8.59	2.08
[66]	Portugal	0.09	0.50	0.78	9.18	1.89
[23]	Portugal	0.11	0.39	1.98	10.84	1.91
[67]	Portugal	0.08	0.56	1.98	10.84	1.91
[68]	Chile	0.06	0.20	1.69	12.69	1.00
[68]	Vietnam	0.13	0.30	0.92	6.49	0.93
[68]	Benin	0.15	0.60	1.16	11.33	0.98
[69]	Australia	0.09	0.30	1.38	8.91	1.05
[70]	France	0.09	0.35	1.77	10.84	2.40
[71]	USA	0.04	0.20	0.85	13.07	1.31
[72]	USA	0.10	0.30	0.39	6.95	0.47

References

1. Stive, M.J.F.; Aarninkhof, S.G.J.; Hamm, L.; Hanson, H.; Larson, M.; Wijnberg, K.M.; Nicholls, R.J.; Capobianco, M. Variability of shore and shoreline evolution. *Coast. Eng.* **2002**, *47*, 211–235. [CrossRef]
2. Labarthe, C.; Castelle, B.; Marieu, V.; Garlan, T.; Bujan, S. Observation and Modeling of the Equilibrium Slope Response of a High-Energy Meso-Macrotidal Sandy Beach. *J. Mar. Sci. Eng.* **2023**, *11*, 584. [CrossRef]
3. Iribarren, C.R. Protection des Ports. In *XVIIth International Navigation Congress*; Permanent International Association of Navigation Congresses: Lisbon, Portugal, 1949; pp. 31–80.
4. Galvin, C.J., Jr. Breaker type classification on three laboratory beaches. *J. Geophys. Res.* **1968**, *73*, 3651–3659. [CrossRef]
5. Battjes, J.A. Surf similarity. *Coast. Eng.* **1974**, *1974*, 466–480.
6. Castelle, B.; Scott, T.; Brander, R.; McCarroll, J.; Robinet, A.; Tellier, E.; De Korte, E.; Simonnet, B.; Salmi, L.-R. Environmental controls on surf zone injuries on high-energy beaches. *Nat. Hazards Earth Syst. Sci.* **2019**, *19*, 2183–2205. [CrossRef]
7. Battjes, J.A.; Bakkenes, H.J.; Janssen, T.T.; van Dongeren, A.R. Shoaling of subharmonic gravity waves. *J. Geophys. Res. Oceans* **2004**, *109*. [CrossRef]
8. Stockdon, H.F.; Holman, R.A.; Howd, P.A.; Sallenger, A.H. Empirical parameterization of setup, swash, and runup. *Coast. Eng.* **2006**, *53*, 573–588. [CrossRef]
9. Melet, A.; Almar, R.; Hemer, M.; Le Cozannet, G.; Meyssignac, B.; Ruggiero, P. Contribution of Wave Setup to Projected Coastal Sea Level Changes. *J. Geophys. Res. Ocean.* **2020**, *125*, e2020JC016078. [CrossRef]
10. Almar, R.; Ranasinghe, R.; Bergsma, E.W.J.; Diaz, H.; Melet, A.; Papa, F.; Kestenare, E. A global analysis of extreme coastal water levels with implications for potential coastal overtopping. *Nat. Commun.* **2021**, *12*, 3775. [CrossRef]
11. Kamphuis, J.W. Alongshore Sediment Transport Rate. *J. Waterw. Port Coast. Ocean. Eng.* **1991**, *117*, 624–640. [CrossRef]
12. Bascom, W.N. The relationship between sand size and beach-face slope. *Trans. Am. Geophys. Union* **1951**, *32*, 866. [CrossRef]
13. Wright, L.D.; Short, A.D.; Green, M.O. Short-term changes in the morphodynamic states of beaches and surf zones: An empirical predictive model. *Mar. Geol.* **1985**, *62*, 339–364. [CrossRef]
14. Buscombe, D.; Masselink, G. Concepts in gravel beach dynamics. *Earth-Sci. Rev.* **2006**, *79*, 33–52. [CrossRef]
15. Ashton, A.; Murray, A.B.; Arnoult, O. Formation of coastline features by large-scale instabilities induced by high-angle waves. *Nature* **2001**, *414*, 296–300. [CrossRef] [PubMed]
16. Roelvink, D.; Huisman, B.; Elghandour, A. Efficient modelling of complex coastal evolution at monthly to century time scales. *Front. Mar. Sci.* **2018**, *7*, 20–23.
17. Roelvink, D.; Reniers, A.; Van Dongeren, A.; Van Thiel De Vries, J.; McCall, R.; Lescinski, J. Modelling storm impacts on beaches, dunes and barrier islands. *Coast. Eng.* **2009**, *56*, 1133–1152. [CrossRef]

18. Van Rijn, L.C. *Principles of Sediment Transport in Rivers, Estuaries and Coastal Seas*; Aqua Publications: Amsterdam, The Netherlands, 1993; 675p.

19. Soulsby, R. *Dynamics of Marine Sands*; T. Telford: London, UK, 1997; 264p.

20. Murray, A.B.; Ashton, A.; Arnoult, O. Large-scale morphodynamic consequences of an instability in alongshore transport. In Proceedings of the Symposium on River, Coastal and Estuarine Morphodynamics, Obihiro, Japan, 10 September 2001.

21. Dean, R.G. *Equilibrium Beach Profiles: US Atlantic and Gulf Coasts*; Department of Civil Engineering, University of Delaware: Newark, Delaware, 1977; Volume 12.

22. Sunamura, T. Quantitative predictions of beach-face slopes. *Geol. Soc. Am. Bull.* **1984**, *95*, 242. [CrossRef]

23. Reis, A.H.; Gama, C. Sand size versus beachface slope—An explanation based on the Constructal Law. *Geomorphology* **2010**, *114*, 276–283. [CrossRef]

24. Muñoz-Pérez, J.J.; Medina, R. Profile changes due to a fortnightly tidal cycle. In Proceedings of the 27th International Conference on Coastal Engineering (ICCE), Sydney, Australia, 16–21 July 2000; pp. 3062–3075.

25. Masselink, G.; Short, A.D. The effect of tide range on beach morphodynamics and morphology: A conceptual beach model. *J. Coast. Res.* **1993**, *9*, 785–800.

26. Muzirafuti, A.; Barreca, G.; Crupi, A.; Faina, G.; Paltrinieri, D.; Lanza, S.; Randazzo, G. The Contribution of Multispectral Satellite Image to Shallow Water Bathymetry Mapping on the Coast of Misano Adriatico, Italy. *J. Mar. Sci. Eng.* **2020**, *8*, 126. [CrossRef]

27. Melet, A.; Teatini, P.; Le Cozannet, G.; Jamet, C.; Conversi, A.; Benveniste, J.; Almar, R. Earth observations for monitoring marine coastal hazards and their drivers. *Surv. Geophys.* **2020**, *41*, 1489–1534. [CrossRef]

28. Benveniste, J.; Mandea, M.; Melet, A.; Ferrier, P. Earth Observations for Coastal Hazards Monitoring and International Services: A European Perspective. *Surv. Geophys.* **2020**, *41*, 1185–1208. [CrossRef]

29. Turner, I.L.; Harley, M.D.; Almar, R.; Bergsma, E.W.J. Satellite optical imagery in Coastal Engineering. *Coast. Eng.* **2021**, *167*, 103919. [CrossRef]

30. Vitousek, S.; Buscombe, D.; Vos, K.; Barnard, P.L.; Ritchie, A.C.; Warrick, J.A. The future of coastal monitoring through satellite remote sensing: Cambridge Prisms. *Coast. Futures* **2023**, *1*, e10. [CrossRef]

31. Yates, M.G.; Jones, A.R.; McGrorty, S.; Goss-Custard, J.D. The Use of Satellite Imagery to Determine the Distribution of Intertidal Surface Sediments of The Wash, England. *Estuar. Coast. Shelf Sci.* **1993**, *36*, 333–344. [CrossRef]

32. Vos, K.; Harley, M.D.; Splinter, K.D.; Simmons, J.A.; Turner, I.L. Sub-annual to multi-decadal shoreline variability from publicly available satellite imagery. *Coast. Eng.* **2019**, *150*, 160–174. [CrossRef]

33. Vos, K.; Harley, M.D.; Splinter, K.D.; Walker, A.; Turner, I.L. Beach slopes from satellite-derived shorelines. *Geophys. Res. Lett.* **2020**, *47*, e2020GL088365. [CrossRef]

34. Cabezas-Rabadán, C.; Pardo-Pascual, J.E.; Palomar-Vázquez, J. Characterizing the relationship between the sediment grain size and the shoreline variability defined from sentinel-2 derived shorelines. *Remote Sens.* **2021**, *13*, 2829. [CrossRef]

35. Carrère, L.; Lyard, F.; Cancet, M.; Guillot, A.; Picot, N. FES 2014, a new tidal model—Validation results and perspectives for improvements. In Proceedings of the ESA Living Planet Symposium, Prague, Czech Republic, 9–13 May 2016; pp. 9–13.

36. Bergsma, E.W.J.; Klotz, A.N.; Artigues, S.; Graffin, M.; Prenowitz, A.; Delvit, J.M.; Almar, R. Shoreliner: A Sub-Pixel Coastal Waterline Extraction Pipeline for Multi-Spectral Satellite Optical Imagery. *Remote Sens.* **2024**, *16*, 2795. [CrossRef]

37. Luijendijk, A.; Hagenaars, G.; Ranasinghe, R.; Baart, F.; Donchyts, G.; Aarninkhof, S. The State of the World's Beaches. *Sci. Rep.* **2018**, *8*, 6641. [CrossRef]

38. McFeeters, S.K. The use of the Normalized Difference Water Index (NDWI) in the delineation of open water features. *Int. J. Remote Sens.* **1996**, *17*, 1425–1432. [CrossRef]

39. Dibarboure, G.; Dorandeu, J.; Le Traon, P.Y.; Picot, N. SSALTO/DUACS: 15 years of precise and consistent multi-mission altimetry data. In Proceedings of the Symposium on 15 Years of Progress in Radar Altimetry, Venice, Italy, 13–18 March 2006; Volume 15.

40. Dee, D.P.; Uppala, S.M.; Simmons, A.J.; Berrisford, P.; Poli, P.; Kobayashi, S.; Andrae, U.; Balmaseda, M.A.; Balsamo, G.; Bauer, P.; et al. The ERA-Interim reanalysis: Configuration and performance of the data assimilation system. *Q. J. R. Meteorol. Soc.* **2011**, *137*, 553–597. [CrossRef]

41. Dean, R.G.; Maurmeyer, E.M. Models for beach profile response. In *Handbook of Coastal Processes and Erosion*; CRC Press: Boca Raton, FL, USA, 2018; pp. 151–166.

42. Almar, R.; Boucharel, J.; Graffin, M.; Abessolo, G.O.; Thoumyre, G.; Papa, F.; Ranasinghe, R.; Montano, J.; Bergsma, E.W.J.; Baba, M.W.; et al. Influence of El Niño on the variability of global shoreline position. *Nat. Commun.* **2023**, *14*, 3133. [CrossRef] [PubMed]

43. Bernabeu, A.M.; Medina, R.; Vidal, C. A morphological model of the beach profile integrating wave and tidal influences. *Mar. Geol.* **2003**, *197*, 95–116. [CrossRef]

44. Kim, H.; Hall, K.; Jin, J.-Y.; Park, G.-S.; Lee, J. Empirical estimation of beach-face slope and its use for warning of berm erosion. *J. Meas. Eng.* **2014**, *2*, 29–42.

45. Bujan, N.; Cox, R.; Masselink, G. From fine sand to boulders: Examining the relationship between beach-face slope and sediment size. *Mar. Geol.* **2019**, *417*, 106012. [CrossRef]

46. Gouzenes, Y.; Léger, F.; Cazenave, A.; Birol, F.; Bonnefond, P.; Passaro, M.; Benveniste, J. Coastal sea level rise at Senetosa (Corsica) during the Jason altimetry missions. *Ocean Sci.* **2020**, *16*, 1165–1182. [CrossRef]

47. Poate, T.; Kingston, K.; Masselink, G.; Russell, P. Response of high-energy, macrotidal beaches to seasonal changes in wave conditions: Examples from North Cornwall, UK. *J. Coast. Res.* **2009**, 747–751. [CrossRef]

48. Garlan, T.; Almar, R.; Gauduin, H.; Gosselin, M.; Morio, O.; Labarthe, C. 3D variability of sediment granulometry in two tropical environments: Nha trang (Vietnam) and saint-Louis (Senegal). *J. Coast. Res.* **2020**, *95*, 495–499. [CrossRef]

49. Garlan, T.; Gabelotaud, I.; Lucas, S.; Marchès, E. A world map of seabed sediment based on 50 years of knowledge. In Proceedings of the 20th International Research Conference, New York, NY, USA, 3–4 June 2018; pp. 3–4.

50. Park, N.W.; Jang, D.H.; Chi, K.H. Integration of IKONOS imagery for geostatistical mapping of sediment grain size at Baramarae beach, Korea. *Int. J. Remote Sens.* **2009**, *30*, 5703–5724. [CrossRef]

51. Rejith, R.G.; Sundararajan, M.; Gnanappazham, L.; Loveson, V.J. Satellite-based spectral mapping (ASTER and landsat data) of mineralogical signatures of beach sediments: A precursor insight. *Geocarto Int.* **2022**, *37*, 2580–2603. [CrossRef]

52. Bergsma, E.W.J.; Almar, R. Coastal coverage of ESA'Sentinel 2 mission. *Adv. Space Res.* **2020**, *65*, 2636–2644. [CrossRef]

53. Salameh, E.; Frappart, F.; Almar, R.; Baptista, P.; Heygster, G.; Lubac, B.; Laignel, B. Monitoring beach topography and nearshore bathymetry using spaceborne remote sensing: A review. *Remote Sens.* **2019**, *11*, 2212. [CrossRef]

54. Mann, S.; Novellino, A.; Hussain, E.; Grebby, S.; Bateson, L.; Capsey, A.; Marsh, S. Coastal Sediment Grain Size Estimates on Gravel Beaches Using Satellite Synthetic Aperture Radar (SAR). *Remote Sens.* **2024**, *16*, 1763. [CrossRef]

55. Salameh, E.; Frappart, F.; Desroches, D.; Turki, I.; Carbonne, D.; Laignel, B. Monitoring intertidal topography using the future SWOT (Surface Water and Ocean Topography) mission. *Remote Sens. Appl. Soc. Environ.* **2021**, *23*, 100578. [CrossRef]

56. Aagaard, T.; Hughes, M.G.; Baldock, T.E.; Power, H.E. Flow dynamics and sediment transport in rip currents. *J. Coast. Res.* **2012**, *28*, 301–309. [CrossRef]

57. Bosom, E.; Jiménez, J.A. Probabilistic coastal vulnerability assessment to storms at regional scale: Application to Catalan beaches (NW Mediterranean). *Nat. Hazards Earth Syst. Sci.* **2011**, *11*, 475–484. [CrossRef]

58. Dingler, J.R. Stability of a very coarse-grained beach at Carmel, California. *Mar. Geol.* **1981**, *44*, 241–252. [CrossRef]

59. Dingler, J.R.; Reiss, T.E. Changes to Monterey Bay beaches from the end of the 1982–83 El Niño through the 1997–98 El Niño. *Mar. Geol.* **2002**, *181*, 249–263. [CrossRef]

60. Gallop, S.L.; Bosserelle, C.; Eliot, I.; Pattiaratchi, C.B. The influence of limestone reefs on storm erosion and recovery of a perched beach. *Cont. Shelf Res.* **2012**, *47*, 16–27. [CrossRef]

61. Guedes RM, C.; Bryan, K.R.; Coco, G.; Holman, R.A. The effects of tides on swash statistics on an intermediate beach. Journal of Geophysical Research. *J. Geophys. Res. Ocean* **2011**, *116*, C04008. [CrossRef]

62. Harris, L.; Nel, R.; Smale, M.; Schoeman, D. Swashed away? Storm impacts on sandy beach macrofaunal communities. *Estuar. Coast. Shelf Sci.* **2011**, *94*, 210–221. [CrossRef]

63. Masselink, G.; Li, L. The role of swash infiltration in determining the beachface gradient: A numerical study. *Mar. Geol.* **2001**, *176*, 139–156. [CrossRef]

64. McLean, R.F.; Kirk, R.M. Relationships between grain size, size-sorting, and foreshore slope on mixed sand-shingle beaches. *N. Z. J. Geol. Geophys.* **1969**, *12*, 138–155. [CrossRef]

65. Mwakumanya, M.A.; Bdo, O. Beach morphological dynamics: A case study of Nyali and Bamburi beaches in Mombasa, Kenya. *J. Coast. Res.* **2007**, *23*, 374–379. [CrossRef]

66. Pinto, C.A.; Taborda, R.; Andrade, C.; Teixeira, S.B. Seasonal and mesoscale variations at an embayed beach (Armacao De Pera, Portugal). *J. Coast. Res.* **2009**, *56*, 118–122.

67. Silva, R.; Baptista, P.; Veloso-Gomes, F.; Coelho, C.; Taveira-Pinto, F. Sediment grain size variation on a coastal stretch facing the North Atlantic (NW Portugal). *J. Coast. Res.* **2009**, *56*, 762–766.

68. Almar, R.; Blenkinsopp, C.; Almeida, L.P.; Bergsma, E.W.J.; Catalan, P.A.; Cienfuegos, R.; Viet, N.T. Intertidal beach profile estimation from reflected wave measurements. *Coast. Eng.* **2019**, *151*, 58–63. [CrossRef]

69. Turner, I.L.; Harley, M.D.; Short, A.D.; Simmons, J.A.; Bracs, M.A.; Phillips, M.S.; Splinter, K.D. A multi-decade dataset of monthly beach profile surveys and inshore wave forcing at Narrabeen, Australia. *Sci. Data* **2016**, *3*, 1–13. [CrossRef]

70. Castelle, B.; Bujan, S.; Marieu, V.; Ferreira, S. 16 years of topographic surveys of rip-channelled high-energy meso-macrotidal sandy beach. *Sci. Data* **2020**, *7*, 410. [CrossRef]

71. Ludka, B.C.; Guza, R.T.; O'Reilly, W.C.; Merrifield, M.A.; Flick, R.E.; Bak, A.S.; Hesser, T.; Bucciarelli, R.; Olfe, C.; Woodward, B.; et al. Sixteen years of bathymetry and waves at San Diego beaches. *Sci. Data* **2019**, *6*, 161. [CrossRef]

72. Larson, M.; Kraus, N.C. Temporal and spatial scales of beach profile change, Duck, North Carolina. *Mar. Geol.* **1994**, *117*, 75–94. [CrossRef]